ChemComm

COMMUNICATION

View Article Online
View Journal | View Issue

Cite this: *Chem. Commun.*, 2016, 52, 4836

Received 4th December 2015,
Accepted 4th March 2016

DOI: 10.1039/c5cc09991a

www.rsc.org/chemcomm

$Ca(BH_4)_2$–Mg_2NiH_4: on the pathway to a $Ca(BH_4)_2$ system with a reversible hydrogen cycle

N. Bergemann,*[a] C. Pistidda,[a] C. Milanese,[b] T. Emmler,[a] F. Karimi,[a] A.-L. Chaudhary,[a] M. R. Chierotti,[c] T. Klassen[ad] and M. Dornheim[a]

The $Ca(BH_4)_2$–Mg_2NiH_4 system presented here is, to the best of our knowledge, the first described $Ca(BH_4)_2$-based hydride composite that reversibly transfers boron from the Ca-based compound(s) to the reaction partner. The ternary boride $MgNi_{2.5}B_2$ is formed upon dehydrogenation and the formation of $Ca(BH_4)_2$ upon rehydrogenation is confirmed.

Due to their high gravimetric H_2 density, metal borohydrides[1] are promising candidates for solid state hydrogen storage. However, high thermal stabilities as well as poor reversibility of their decomposition products are the major obstacles to be overcome for technical applications. One of the most promising approaches to solve the reversibility issue of borohydrides is to combine them with selected materials to create reversible reactive compositions with lowered reaction enthalpy, the so-called reactive hydride composites (RHCs).[2,3] The system that has attracted the most attention in recent years is $LiBH_4$–MgH_2.[4] Because of its reduced desorption enthalpy compared to $LiBH_4$, mixtures of hydrides based on $Ca(BH_4)_2$ were also investigated intensively. Unfortunately, all systems presented so far have suffered from sluggish hydrogen reaction kinetics and poor reversibility. One reason for the latter finding is the tendency of $Ca(BH_4)_2$ to form kinetically stable side products upon dehydrogenation that hinder a complete rehydrogenation. In the case of pure $Ca(BH_4)_2$, several desorption paths are proposed in the literature:

$$Ca(BH_4)_2 \rightarrow CaH_2 + 2B + 3H_2\ ^{5-7} \quad (1)$$

$$Ca(BH_4)_2 \rightarrow 2/3CaH_2 + 1/3CaB_6 + 10/3H_2\ ^{5,6,8-10} \quad (2)$$

$$Ca(BH_4)_2 \rightarrow 1/6CaB_{12}H_{12} + 5/6CaH_2 + 13/6H_2\ ^{9-11} \quad (3)$$

$$Ca(BH_4)_2 \rightarrow CaB_2H_6 + H_2 \text{ (intermediate reaction)}.^{6,10,11} \quad (4)$$

In fact, recent reports have indicated that the decomposition of $Ca(BH_4)_2$ may follow more than one single reaction path.[6,12] In these studies, the respective decomposition products and their ratio partially depend on the applied hydrogen back-pressure as well as the dehydrogenation temperature.[6,12]

Also for the hydride composite $Ca(BH_4)_2$–MgH_2,[8,13–16] several possible decomposition pathways are reported in the literature:

$$Ca(BH_4)_2 + MgH_2 \rightarrow CaH_2 + MgB_2 + 4H_2\ ^{8} \quad (5)$$

$$Ca(BH_4)_2 + MgH_2 \rightarrow 2/3CaH_2 + 1/3CaB_6 + Mg + 13/3H_2\ ^{8,13} \quad (6)$$

$$Ca(BH_4)_2 + MgH_2 \rightarrow 1/6CaB_{12}H_{12} + 5/6CaH_2 + Mg + 19/6H_2.^{13} \quad (7)$$

For this system, Bonatto-Minella *et al.* demonstrated a reversibility of approximately 55% between subsequent cycles.[15] The authors rule out the possibility that the hydride composite desorbs according to eqn (5). Instead, the formation of CaB_6 was confirmed to be the cause of the partial reversibility (eqn (6)), which was also reported earlier by Kim *et al.*[8,16] Bonatto-Minella *et al.* suggested that Mg promotes a better reversibility of the composite compared to pure $Ca(BH_4)_2$ by acting as a nucleation agent for CaB_6 due to the low *d*-value mismatch $\{111\}_{CaB_6}/\{1011\}_{Mg}$ of only 0.6%.[15] Consequently, this mixture cannot be considered as a typical RHC since the overall desorption enthalpy is not lowered by the formation of reaction products between $Ca(BH_4)_2$ (including its decomposition products) and Mg/MgH_2. The drop in reversible capacity is attributed to the formation of $CaB_{12}H_{12}$ which has too high kinetic barriers to reversibly form $Ca(BH_4)_2$ under moderate temperature and hydrogen pressure conditions.[13] Therefore, this kinetically stable phase acts as a boron sink upon cycling.

In order to obtain complete reversibility for $Ca(BH_4)_2$-based systems, a reaction partner has to be identified that can reversibly and effectively bind boron, hence preventing the formation of competing stable phases like $CaB_{12}H_{12}$ or amorphous boron. This compound should be lightweight and preferably store hydrogen itself. Mg_2NiH_4,[17–20] which has a hydrogen capacity of 3.6 mass%, matches these criteria. Vajo *et al.* showed that a mixture of $LiBH_4$ and Mg_2NiH_4 forms the ternary boride $MgNi_{2.5}B_2$ upon desorption

[a] *Helmholtz-Zentrum Geesthacht, Institute of Materials Research, Max-Planck-Strasse 1, D-21502 Geesthacht, Germany. E-mail: nils.bergemann@hzg.de*
[b] *Pavia H_2 Lab, C.S.G.I. & Dipartimento di Chimica, Sezione di Chimica Fisica, Universitá di Pavia, Viale Taramelli 16, I-27100 Pavia, Italy*
[c] *Department of Chemistry and NIS Centre, University of Torino, V. P. Giuria 7, I–10125 Torino, Italy*
[d] *Helmut Schmidt University, Mechanical Engineering, Holstenhofweg 85, D-22043 Hamburg, Germany*

which can act as boron donor to form $LiBH_4$ again.[21,22] Later Afonso *et al.* confirmed a similar reaction mechanism for the composite $NaBH_4$–Mg_2NiH_4.[23]

In this work, the dehydrogenation reactions of the system $Ca(BH_4)_2$–Mg_2NiH_4 have been investigated for the first time. Furthermore, the potential for complete rehydrogenation of the desorbed products is demonstrated. For all experiments shown in this work, an initial mixture of $Ca(BH_4)_2$ and Mg_2NiH_4 in a molar ratio of 1 : 2.5 was prepared by 5 hours of ball milling.† To investigate the thermal dehydrogenation path, an *in situ* synchrotron radiation powder X-ray diffraction (SR-PXD) experiment was performed applying a temperature ramp of 5 K min^{-1} heating from ambient temperature to 450 °C at 1 bar H_2 (Fig. 1). The room temperature diffraction pattern exhibits the diffraction peaks of the low-temperature monoclinic phase ($C12/c1$) of Mg_2NiH_4 and its high-temperature cubic phase ($Fm\bar{3}m$) (weight ratio approx. 2.3 : 1). Diffraction peaks of $Ca(BH_4)_2$ can be attributed to the α-($F2dd$) and γ-phase ($Pbca$), with a weight ratio of roughly 5 : 1. The first event with rising temperature is the polymorphous change from α-/γ-$Ca(BH_4)_2$ to β-$Ca(BH_4)_2$ ($P\bar{4}$), which starts at about 174 °C. The second modification in the diffraction pattern is related to another polymorphous change: the monoclinic Mg_2NiH_4 converts to the cubic phase at approx. 244 °C. At about 318 °C, Mg_2NiH_4 starts to decompose to Mg_2Ni and hydrogen. At slightly higher temperatures, the intensity of $Ca(BH_4)_2$ diffraction peaks starts to decrease, while the peaks of four other phases occur and intensify, namely $MgNi_{2.5}B_2$, Mg, CaH_2 and an unknown phase. With further temperature increase, the peaks of Mg_2Ni first grow until the maximum intensity is reached at roughly 365 °C, followed by a quick decline of peak intensity. The peaks of $MgNi_{2.5}B_2$, Mg and CaH_2 grow during the remaining heating period and the following isothermal region at 450 °C. In contrast, the peaks of the unknown phase only grow until the highest intensity is attained at about

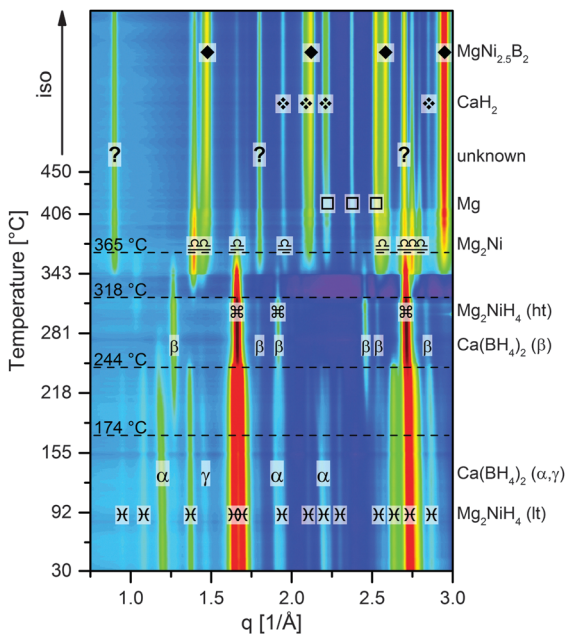

Fig. 1 *In situ* SR-PXD analysis of $Ca(BH_4)_2$–Mg_2NiH_4, the sample was heated at 5 K min^{-1} from RT to 450 °C at 1 bar H_2.

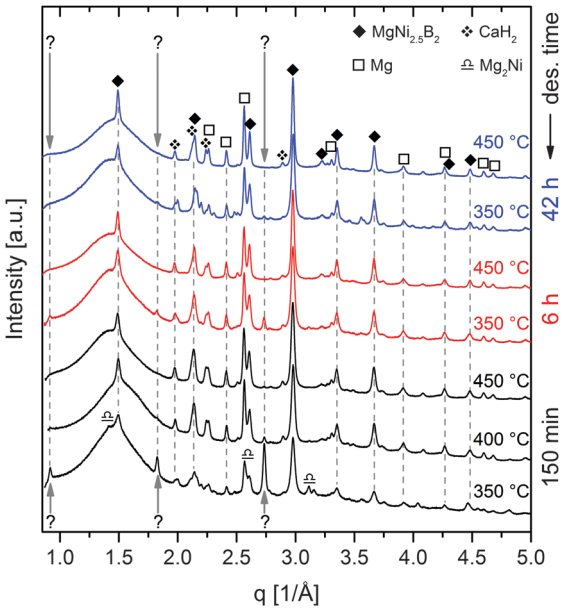

Fig. 2 *Ex situ* PXD pattern of $Ca(BH_4)_2$–Mg_2NiH_4 desorbed at 1 bar H_2 and different final temperatures and times, respectively.

410 °C, then the peak intensities reduce much slower than those of Mg_2Ni. Moreover, it must be emphasised that the diffraction peaks of $Ca(BH_4)_2$ vanish already at about 365 °C, that is when $MgNi_{2.5}B_2$ and the unknown phase, which potentially contains boron, are still growing. This finding strongly suggests the possibility of Mg_2Ni reacting with the decomposition products of $Ca(BH_4)_2$, *i.e.* CaB_6, CaB_xH_y and/or amorphous boron. Furthermore, the sequence of peak intensity changes for the different phases suggests that the unknown phase is a yet unreported Mg–Ni–B-phase. Since the reaction kinetics for the dehydrogenation are too sluggish to monitor the complete process by means of *in situ* SR-PXD, additional material was desorbed at a pressure of 1 bar H_2 in a Sieverts apparatus and then characterised using *ex situ* laboratory Powder X-ray Diffraction (PXD). Fig. 2 shows the diffraction patterns‡ of seven different samples. All samples were heated to their respective maximum temperatures with 3 K min^{-1}; subsequently the material was kept under isothermal conditions for different times. Diffractograms with the same colour represent samples with equal total desorption time, *i.e.* the isothermal time was altered in such a manner that the overall time of both, heating period and isotherm, was equal for desorptions of the same set. Diffractograms of samples with a total desorption time of 150 minutes are shown in black. Red and blue diffractograms indicate total desorption times of 6 and 42 hours, respectively. The sample heated up to 350 °C for 150 min shows the peaks of Mg_2Ni and the unknown phase besides those of $MgNi_{2.5}B_2$, Mg and CaH_2. However, compared to the *in situ* SR-PXD pattern at 350 °C the ratios of the individual phases are different: Mg_2Ni almost vanished whereas the peaks of the unknown phase are much more pronounced than at any temperature in the *in situ* experiment. Hence, it can be deduced that the reaction path leading to this unknown phase is more dominant at lower temperatures. Nevertheless, looking at the PXD patterns of the material desorbed at 350 °C with longer isotherms, the peaks of the unknown phase first decline (6 h)

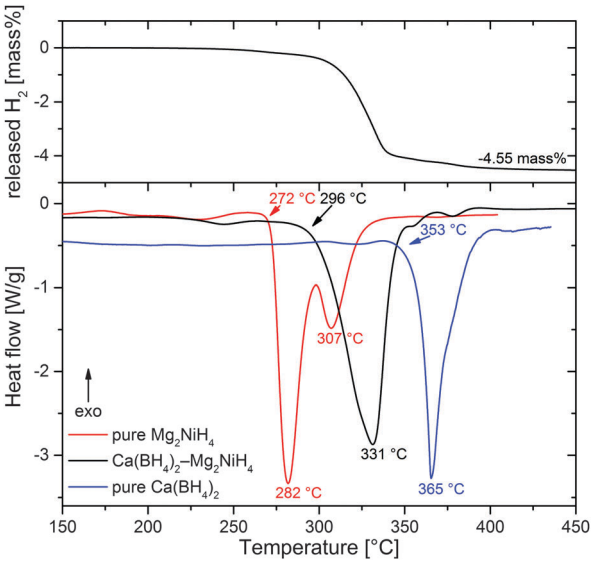

Fig. 3 Combined DSC and volumetric analyses of $Ca(BH_4)_2$–Mg_2NiH_4, diagrams of pure Mg_2NiH_4 and $Ca(BH_4)_2$ are included for reference.

and eventually vanish (42 h). Heating the composite to 450 °C results in the complete disappearance of the unknown phase already within the short isothermal period. Therefore, independent of temperature, this unknown phase clearly cannot be an end product but is an intermediate phase in this reaction. Thus, the overall desorption reaction can be summarised in the following chemical equation:

$$Ca(BH_4)_2 + 2.5Mg_2NiH_4 \rightarrow CaH_2 + MgNi_{2.5}B_2 + 4Mg + 8H_2. \quad (8)$$

The quantity of hydrogen released in this desorption reaction amounts to 4.6 mass%.

Fig. 3 presents results of Differential Scanning Calorimetry (DSC) combined with volumetric analysis for $Ca(BH_4)_2$–Mg_2NiH_4 in comparison to pure Mg_2NiH_4 and $Ca(BH_4)_2$ (all materials ball milled using the same parameters), obtained under 1 bar H_2 and a heating rate of 5 K min^{-1}. The composite shows one broad endothermic desorption peak (onset at 296 °C, maximum at 331 °C) that embraces the several sub-events. This is in agreement with the *in situ* SR-PXD experiment which revealed that the desorption of Mg_2NiH_4 triggers the described follow-up reactions and that the partial reactions overlap in time. Compared to pure $Ca(BH_4)_2$ (onset 353 °C, maximum 365 °C), desorption temperatures are shifted to lower values by about 55 K in the case of the composite. Thus, Mg_2NiH_4 or, more specifically, Mg$_2$Ni clearly destabilises $Ca(BH_4)_2$. However, pure Mg_2NiH_4§ (onset 272 °C, first maximum 282 °C) starts to dehydrogenate at temperatures lower than those for $Ca(BH_4)_2$–Mg_2NiH_4. This discrepancy must be attributed to the kinetic limitations of Mg_2NiH_4 decomposition in the RHC with respect to pure Mg_2NiH_4. A possible explanation could be a reduced energy transfer to Mg_2NiH_4 upon ball milling due to the cushioning effect of $Ca(BH_4)_2$. As a consequence, the Mg_2NiH_4 within the composite would have higher activation barriers for desorption as compared to the pure Mg_2NiH_4. In comparison, the temperatures in the DSC experiments are roughly 20 K lower than in the *in situ* SR-PXD measurements. This deviation may be due to the particular experimental setup of SR-PXD experiments, where an inevitable gap between the specimen and the thermocouple may cause a temperature offset. At 4.55 mass%, the amount of released hydrogen agrees well with the theoretical capacity of the RHC of 4.6 mass%.

In order to investigate the possible presence of boron-containing phases that are not detectable using X-ray diffraction – $CaB_{12}H_{12}$ and B are typically nano-crystalline or amorphous[7,11,13] – ^{11}B Magic Angle Spinning Nuclear Magnetic Resonance (MAS-NMR) spectroscopy was employed. The spectra of the as-milled material and of the material desorbed for 24 h at 450 °C and dynamic H_2 pressure of more than 1 bar can be found in Fig. 4 (black and red graphs). As can be seen, the initial material comprises only one boron-containing phase, that is $Ca(BH_4)_2$. More precisely, the peak at −32.2 ppm is a convolution of α- and γ-$Ca(BH_4)_2$. The desorbed sample features one peak at 141.6 ppm which is assigned to $MgNi_{2.5}B_2$. This result is quite remarkable since it shows that none of the typical decomposition products of $Ca(BH_4)_2$ could be detected in the desorbed state. Instead, all boron seems to be bonded in the form of $MgNi_{2.5}B_2$. Since the formation of the kinetically stable phases $CaB_{12}H_{12}$ and/or B is the main reason for the degradation of $Ca(BH_4)_2$-based systems, the absence of these phases may allow for full reversibility of a $Ca(BH_4)_2$-based H_2 storage material. Consequently, the reabsorption potential of the $Ca(BH_4)_2$–Mg_2NiH_4 composite was evaluated. The decomposition products were kept in an autoclave under hydrogen with an initial pressure of 395 bar¶ and a temperature of 400 °C for 14 h. These high pressure hydrogenation conditions were chosen arbitrarily in an attempt to maximise the potential conversion of the decomposition products into the starting material. The NMR spectrum of the reabsorbed sample is shown in Fig. 4 (blue graph). There are two major resonance peaks: the first at 141.5 ppm can be assigned to $MgNi_{2.5}B_2$, the second, at −32.6 ppm, clearly belongs to $Ca(BH_4)_2$. Since the desorbed sample only features $MgNi_{2.5}B_2$ as the sole boron-containing phase, the $Ca(BH_4)_2$ formed must have received the boron from this ternary boride upon

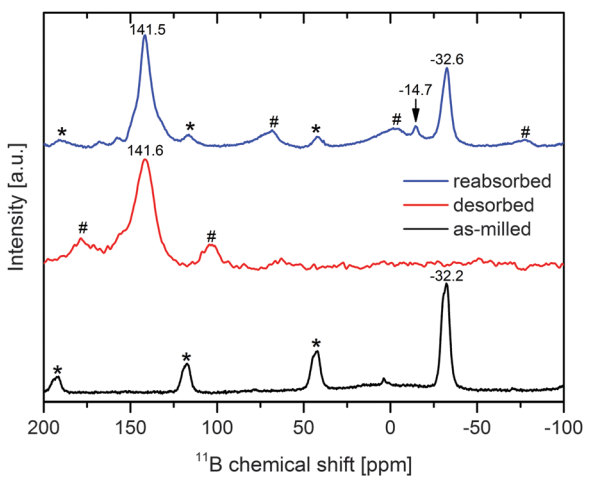

Fig. 4 ^{11}B MAS-NMR spectra of as-milled $Ca(BH_4)_2$–Mg_2NiH_4 (black), desorbed $Ca(BH_4)_2$–Mg_2NiH_4 (red) and of the reabsorbed material (blue), sidebands of $Ca(BH_4)_2$ and $MgNi_{2.5}B_2$ are marked with * and #, respectively.

absorption. Consequently, aside from its ability to act as a boron-donor for the formation of $LiBH_4$ and $NaBH_4$, $MgNi_{2.5}B_2$ also exchanges boron reversibly with $Ca(BH_4)_2$. The ^{11}B spectrum of the reabsorbed material also shows another small resonance peak at −14.7 ppm which cannot be assigned clearly. However, it can be assumed that it belongs to a $(B_xH_y)^{z-}$-phase that could be an intermediate product in $Ca(BH_4)_2$ formation. The NMR spectrum indicates a converted fraction to $Ca(BH_4)_2$ of roughly one-third. However, the reabsorption did not complete under the applied conditions since there is still a high fraction of $MgNi_{2.5}B_2$ present in the absorbed sample. At the moment the reason for this limited reconversion is not clear yet. Since the PXD analysis of the reabsorbed sample (not presented here) only shows very small and broad $Ca(BH_4)_2$ reflexes, the $Ca(BH_4)_2$ crystallites seem to be rather small. Hence, crystallite growth appears to be restricted. Further studies will have to clarify which microstructure develops and whether the reconversion into the initial hydride is confined in some way. For instance, the reconversion may be restricted to interface areas between the desorbed reactants, and the newly formed $Ca(BH_4)_2$ may act as a diffusion barrier, leading to reduced kinetic rates and thus an incomplete rehydrogenation.

In summary, the reactive hydride composite $Ca(BH_4)_2$–Mg_2NiH_4 features a complete boron transfer from $Ca(BH_4)_2$ to $MgNi_{2.5}B_2$ upon dehydrogenation. No other boron-containing phases were present among the decomposition products; this includes especially the inactive phases amorphous boron and $CaB_{12}H_{12}$. Hence, a degradation of the hydrogen storage capacity caused by these boron sinks, as observed in pure $Ca(BH_4)_2$[6,7,11] or $Ca(BH_4)_2$–MgH_2,[13–15,24] can be ruled out for this composite. Mg_2NiH_4 destabilises $Ca(BH_4)_2$ at a hydrogen pressure of 1 bar resulting in the lowering of desorption temperatures by about 55 K as compared to pure $Ca(BH_4)_2$. These dehydrogenation conditions might still be above the desired temperature range for technical applications. However, the absence of boron sinks must be considered as a substantial improvement of $Ca(BH_4)_2$ based RHCs. Further optimisation of the material preparation should reduce the desorption temperatures at least down to the level of Mg_2NiH_4. Although the system did not reabsorb entirely, it was proven that the formation of $Ca(BH_4)_2$ starting from $MgNi_{2.5}B_2$ as boron-donor is thermodynamically and kinetically possible. Reabsorption conditions have not been optimised yet. Hence, it is likely that rehydrogenation could also be achieved at lower temperatures and pressure. Moreover, no additives were used within this study. Therefore, further improvements of the hydrogen sorption kinetics may be feasible.

This work was supported by the Danish Council for Strategic Research *via* HyFillFast. Access to beam time at the synchrotron PETRA III at DESY, Hamburg, Germany is gratefully acknowledged.

Notes and references

† The milling was performed in a SPEX 8000M Mill using stainless steel milling vials and stainless steel balls with a diameter of 10 mm. A ball-to-powder ratio of 10 : 1 was employed.

‡ The background of each diffraction pattern has a broad amorphous peak between 1 and 2 $Å^{-1}$ which is caused by the PMMA sample holder used to protect the material from air.

§ Typically, Mg_2NiH_4 features only one single desorption peak. The presence of the double peak is a kinetic effect. A possible explanation could be a kinetic separation between nucleation and growth of Mg_2Ni[25] as a consequence of the rather low activation energy for desorption and a rather homogeneous particle size distribution after 5 h of ball milling.

¶ Due to absorption and a small leakage the pressure dropped to approx. 180 bar at the end of the synthesis.

1 H.-W. Li, Y. Yan, S. Orimo, A. Züttel and C. M. Jensen, *Energies*, 2011, **4**, 185–214.
2 M. Dornheim, S. Doppiu, G. Barkhordarian, U. Boesenberg, T. Klassen, O. Gutfleisch and R. Bormann, *Scr. Mater.*, 2007, **56**, 841–846.
3 G. Barkhordarian, T. Klassen, M. Dornheim and R. Bormann, *J. Alloys Compd.*, 2007, **440**, L18–L21.
4 U. Bösenberg, S. Doppiu, L. Mosegaard, G. Barkhordarian, N. Eigen, A. Borgschulte, T. R. Jensen, Y. Cerenius, O. Gutfleisch, T. Klassen, M. Dornheim and R. Bormann, *Acta Mater.*, 2007, **55**, 3951–3958.
5 J. H. Kim, S. A. Jin, J. H. Shim and Y. W. Cho, *J. Alloys Compd.*, 2008, **461**, 2007–2009.
6 Y. Yan, A. Remhof, D. Rentsch, A. Züttel, S. Giri and P. Jena, *Chem. Commun.*, 2015, **51**, 11008–11011.
7 C. Bonatto Minella, S. Garroni, C. Pistidda, G. Barkhordarian, C. Rongeat, I. Lindemann, O. Gutfleisch, T. R. Jensen, Y. Cerenius, J. Christensen, M. D. Bar, T. Klassen and M. Dornheim, *J. Phys. Chem. C*, 2011, **115**, 2497–2504.
8 Y. Kim, D. Reed, Y.-S. Lee, J. Y. Lee, J.-H. Shim, D. Book and Y. W. Cho, *J. Phys. Chem. C*, 2009, **113**, 5865–5871.
9 V. Ozolins, E. H. Majzoub and C. Wolverton, *J. Am. Chem. Soc.*, 2009, **131**, 230–237.
10 Y. Zhang, E. Majzoub, V. Ozoliņš and C. Wolverton, *Phys. Rev. B: Condens. Matter Mater. Phys.*, 2010, **82**, 174107.
11 Y. Kim, S. J. Hwang, J. H. Shim, Y. S. Lee, H. N. Han and Y. W. Cho, *J. Phys. Chem. C*, 2012, **116**, 4330–4334.
12 Y. Kim, S. Hwang, Y. Lee, J. Suh, H. N. Han and Y. W. Cho, *J. Phys. Chem. C*, 2012, **116**, 25715–25720.
13 C. Bonatto Minella, S. Garroni, D. Olid, F. Teixidor, C. Pistidda, I. Lindemann, O. Gutfleisch, M. D. Bar, R. Bormann, T. Klassen and M. Dornheim, *J. Phys. Chem. C*, 2011, **115**, 18010–18014.
14 F. Karimi, P. K. Pranzas, A. Hoell, U. Vainio, E. Welter, V. S. Raghuwanshi, C. Pistidda, M. Dornheim, T. Klassen and A. Schreyer, *J. Appl. Crystallogr.*, 2014, **47**, 67–75.
15 C. B. Minella, C. Pistidda, S. Garroni, P. Nolis, M. D. Baró, O. Gutfleisch, T. Klassen, R. Bormann and M. Dornheim, *J. Phys. Chem. C*, 2013, **117**, 3846–3852.
16 Y. Kim, D. Reed, Y.-S. Lee, J.-H. Shim, H. N. Han, D. Book and Y. W. Cho, *J. Alloys Compd.*, 2010, **492**, 597–600.
17 K. Zeng, T. Klassen, W. Oelerich and R. Bormann, *J. Alloys Compd.*, 1999, **283**, 213–224.
18 Z. Gavra, M. H. Mintz, G. Kimmel and Z. Hadari, *Inorg. Chem.*, 1979, **18**, 3595–3597.
19 T. Hirata, T. Matsumoto, M. Amano and Y. Sasaki, *J. Phys. F: Met. Phys.*, 1981, **11**, 521–529.
20 M. Polanski, T. K. Nielsen, I. Kunce, M. Norek, T. Płociński, L. R. Jaroszewicz, C. Gundlach, T. R. Jensen and J. Bystrzycki, *Int. J. Hydrogen Energy*, 2013, **38**, 4003–4010.
21 J. J. Vajo, W. Li and P. Liu, *Chem. Commun.*, 2010, **46**, 6687–6689.
22 W. Li, J. J. Vajo, R. W. Cumberland, P. Liu, S. J. Hwang, C. Kim and R. C. Bowman, *J. Phys. Chem. Lett.*, 2010, **1**, 69–72.
23 G. Afonso, A. Bonakdarpour and D. P. Wilkinson, *J. Phys. Chem. C*, 2013, **117**, 21105–21111.
24 C. Bonatto Minella, S. Garroni, C. Pistidda, M. D. Baró, O. Gutfleisch, T. Klassen and M. Dornheim, *J. Alloys Compd.*, 2015, **622**, 989–994.
25 T. Klassen, U. Herr and R. S. Averback, *Acta Mater.*, 1997, **45**, 2921–2930.